



Cite this: *Chem. Commun.*, 2016, 52, 5872

Received 24th February 2016,  
Accepted 22nd March 2016

DOI: 10.1039/c6cc01686c

www.rsc.org/chemcomm

## Differently sized magnetic/upconversion luminescent NaGdF<sub>4</sub>:Yb,Er nanocrystals: flow synthesis and solvent effects†

Mingxia Jiao, Lihong Jing, Chunyan Liu, Yi Hou, Jiayi Huang, Xiaojun Wei and Mingyuan Gao\*

**The present study reports a novel approach for synthesizing differently sized magnetic/upconversion luminescent NaGdF<sub>4</sub>:Yb,Er nanocrystals through flow chemistry. The solvent effects on the control of particle size were particularly investigated for tailoring the size and physical properties of the resulting particles potentially useful for bioimaging.**

Rare-earth (RE) nanocrystals have attracted increasing attention owing to the unique magnetic and upconversion luminescent properties useful for versatile biological and biomedical applications.<sup>1–5</sup> Apart from the outstanding performance as contrast agents in magnetic resonance imaging (MRI), especially for tumor imaging,<sup>6–9</sup> NaGdF<sub>4</sub> nanocrystals have been demonstrated to be a suitable host for Ln<sup>3+</sup> emitting dopants, due to the low phonon energy, to achieve upconversion luminescence that locates at shorter wavelength than the near-infrared excitation.<sup>7,8</sup> For example, PEGylated Yb<sup>3+</sup>/Er<sup>3+</sup> co-doped NaGdF<sub>4</sub> nanoparticles exhibiting vivid green emissions have been adopted for tiny tumor imaging and surgical navigation as well.<sup>7,10</sup>

Driven by these appealing biomedical applications, the synthesis of doped NaGdF<sub>4</sub> nanocrystals with size-/composition-dependent physical properties has been intensively investigated in the past decade.<sup>1,11,12</sup> The synthetic route based on replacement reactions taking place at high temperature has been demonstrated to be more effective and flexible.<sup>7,8,13,14</sup> It allows differently 2.0–19.8 nm NaGdF<sub>4</sub> nanocrystals to be achieved by adjusting the reaction temperature and time for the nucleation and growth processes,<sup>8,13,15</sup> and 5.0–36.7 nm NaGdF<sub>4</sub>:Yb,Er (quasi-)spherical nanocrystals by varying the reaction time or reactant ratios of F<sup>-</sup>:Ln<sup>3+</sup> and Na<sup>+</sup>:Ln<sup>3+</sup>.<sup>7,16</sup> However, upconversion NaGdF<sub>4</sub>:Yb,Er nanocrystals below 10 nm remain difficult to obtain.<sup>11</sup> This is because hexagonally phased NaGdF<sub>4</sub>, as the matrix for

the emitting dopants, is essentially required while the cubic phase is typically dominant in this size regime. Moreover, the pharmacokinetic behaviors are strongly correlated with the particle size, and small particles present shorter biological half-lives.<sup>7</sup> It is therefore meaningful to explore the synthesis of upconversion luminescent and magnetic bifunctional nanoparticles smaller than 10 nm for biomedical applications, yet remains challenging.

On the other hand, the previous synthesis studies on NaGdF<sub>4</sub> nanoparticles were mainly based on conventional batch reactions, while the poor batch-to-batch reproducibility may set a huge hurdle for practical applications. Fortunately, new-emerging flow chemistry may offer a satisfying solution,<sup>17</sup> but the flow synthesis of magnetic and upconversion luminescent NaGdF<sub>4</sub> nanoparticles has not been reported so far.

On the basis of our previous investigations on the batch-based synthesis of NaGdF<sub>4</sub> nanocrystals and the flow synthesis of biocompatible iron oxide nanoparticles,<sup>6–8,17</sup> herein we report a flow synthesis of magnetic/upconversion luminescent NaGdF<sub>4</sub>:Yb,Er nanocrystals smaller than 10 nm. Benefiting from the high pressure of the flow reaction system, different types of low boiling point solvents were allowed for investigating the impacts of solvent viscosity and solvation ability on the size and optical properties of the resulting particles. In addition, the associated kinetics and thermodynamics aspects were also discussed.

In brief, NaGdF<sub>4</sub>:Yb,Er nanocrystals were continuously prepared using a 1.0 mm tube reactor at 260 °C under a pressure of 30 bar, maintained automatically with a computer-controlled synthetic system. The residence time was 30 min. Typically, 0.80 mmol GdCl<sub>3</sub>·6H<sub>2</sub>O, 0.18 mmol YbCl<sub>3</sub>·6H<sub>2</sub>O, 0.02 mmol ErCl<sub>3</sub>·6H<sub>2</sub>O, 2.5 mmol NaOH and 4.0 mmol NH<sub>4</sub>F were used as precursors, and 14 mL oleic acid (OA) was used as both a particle surface capping agent and co-solvent together with 16 mL 1-octadecene (ODE). The above recipe was previously optimized with respect to upconversion luminescence based on batch preparation.<sup>7</sup> Different to the previous method, low boiling point solvents such as cyclohexane or methanol were

*Institute of Chemistry, Chinese Academy of Sciences, Bei Yi Jie 2, Zhong Guan Cun, Beijing 100190, China. E-mail: gaomy@iccas.ac.cn; Web: www.gaomingyuan.com; Fax: +86 10 8261 3214*

† Electronic supplementary information (ESI) available: (1) Experimental details, (2) characterization of the flow synthesized NaGdF<sub>4</sub>:Yb,Er nanocrystals, (3) analysis of the diffusion coefficient. See DOI: 10.1039/c6cc01686c



Scheme 1 Sketch of the flow synthesis of NaGdF<sub>4</sub>:Yb,Er nanocrystals.

added into the stock solutions for tuning the particle size. The continuous synthesis is schematically shown in Scheme 1. The as-prepared NaGdF<sub>4</sub>:Yb,Er nanocrystals prepared in the absence of any low boiling point solvents are quasi-spherical as shown in Fig. 1a. The average size is of 4.3 nm and the relative standard deviation (RSD) is around 7.0% (Fig. S1a, ESI<sup>†</sup>). The electron diffraction (ED) analysis shown in the inset of Fig. 1a suggests that the as-prepared NaGdF<sub>4</sub>:Yb,Er particles are in hexagonal phase<sup>18</sup> and possess high crystallinity as indicated by the intense diffraction rings, which may result from the high pressure of the reaction system.

The upconversion luminescence of NaGdF<sub>4</sub>:Yb,Er nanocrystals is known to be strongly dependent on the particle size.<sup>1,7</sup> Our previous study revealed that the particle size can only be varied in a limited range of 4.2–6.8 nm for biocompatible iron oxide nanoparticles. However, the systematic studies suggested that the particle growth is strongly correlated with the diffusion coefficient of the monomer and particle nuclei in the solvent.<sup>17</sup> Therefore, the low boiling point solvent cyclohexane was introduced into the stock solution before it was pumped into the tube reactor. In the presence of 10 mL cyclohexane, the average size is effectively increased to 6.1 nm as shown in Fig. 1b. Meanwhile, the RSD is decreased to 6.6% (Fig. S1b, ESI<sup>†</sup>). More importantly, the resulting particles are also in hexagonal phase, demonstrated by ED. To rule out any dilution effect on the particle size, an equal amount of ODE was introduced instead of cyclohexane into the stock solution prior to the preparation of the NaGdF<sub>4</sub>:Yb,Er nanocrystals. The particles obtained under the same preparative conditions, as displayed in Fig. S2 (ESI<sup>†</sup>), are nearly identical to those shown in Fig. 1a. Therefore, the effective size increase induced by cyclohexane can be attributed to the reduced viscosity of the mixed solvents. For example, the viscosity of the mixed solvent ( $V_{\text{cyclohexane}}:V_{\text{ODE/OA}} = 1:3$ ) is of 4.7 mPa s, sufficiently lower than that (11.5 mPa s) for the ODE/OA mixture at 20 °C. According to Einstein's formula (ESI<sup>†</sup>), the diffusion coefficient of the solute is inversely correlated with the viscosity of the solvent. In consequence of the reduced viscosity of the solvent, the nanocrystal growth rate will be increased and particle size distribution will be decreased if a diffusion-controlled growth is dominant.<sup>19,20</sup>

For tuning the particle size, apart from the diffusion coefficient of precursor/monomer and nuclei, the precursor/monomer saturation also plays an important role in both nucleation and the following growth processes, which is closely related with the solvation ability of solvent.<sup>21</sup> Therefore, methanol was selected below as a low boiling point solvent, as it is a good solvent for all the precursors including GdCl<sub>3</sub>, YbCl<sub>3</sub>, ErCl<sub>3</sub>, NaOH and NH<sub>4</sub>F for achieving NaGdF<sub>4</sub>:Yb,Er nanocrystals, for further

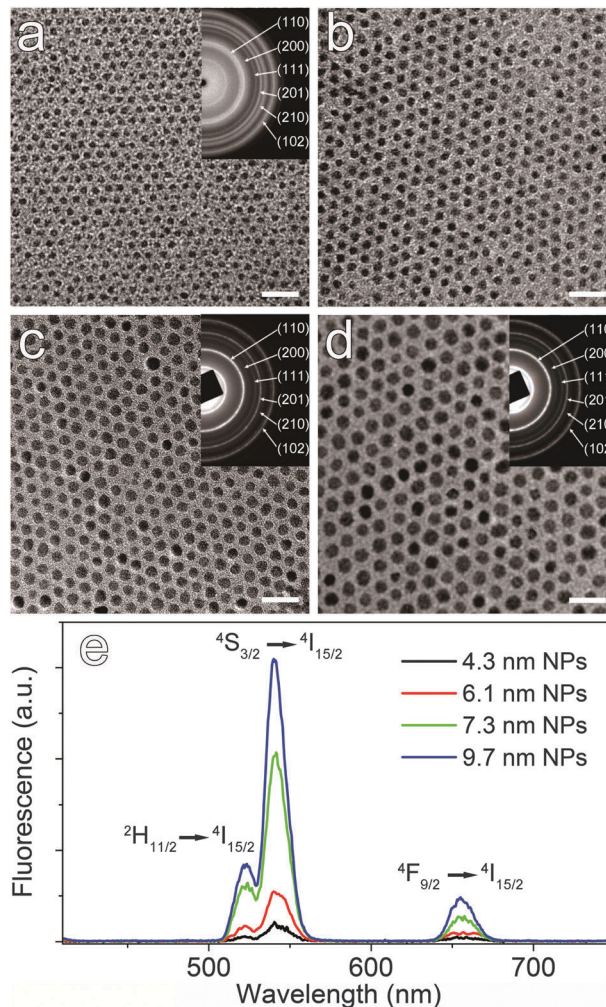


Fig. 1 Transmission electron microscopy (TEM) images of NaGdF<sub>4</sub>:Yb,Er nanocrystals prepared in the absence of any low boiling point solvent (a), in the presence of 10 mL cyclohexane (b), 5 mL methanol (c), or 10 mL methanol (d) (the scale bars correspond to 25 nm), with electron diffraction pattern overlaid with the identification of different diffraction rings labeled with Miller indices of hexagonal NaGdF<sub>4</sub> according to JCPDS card (27-0699). The lower frame (e) shows the upconversion luminescence spectra of the as-prepared NaGdF<sub>4</sub>:Yb,Er nanocrystals (frames a–d) in cyclohexane recorded upon excitation by a CW 980 nm laser.

increasing the size of the resulting particles. As expected, 5 mL and 10 mL methanol can further increase the particle size up to  $7.3 \pm 0.6$  nm and  $9.7 \pm 0.7$  nm, respectively, as shown in Fig. 1c and d. Apart from maintaining the particle monodispersity well (Fig. S1, ESI<sup>†</sup>), the hexagonally phased particles remain highly crystalline, rather comparable with those obtained in the presence of cyclohexane, as indicated by the ED patterns shown as inset of Fig. 1c and d.

Apart from the improved diffusion coefficient arising from the reduced viscosity, *e.g.*, 5.7 and 3.7 mPa s for 5 and 10 mL methanol-containing systems, from the thermodynamics aspect, the increased solubility of all the precursors in the reaction system reduces the amount of precursors consumed during the nucleation process due to the reduced supersaturation degree, which is consequently favorable for growing larger

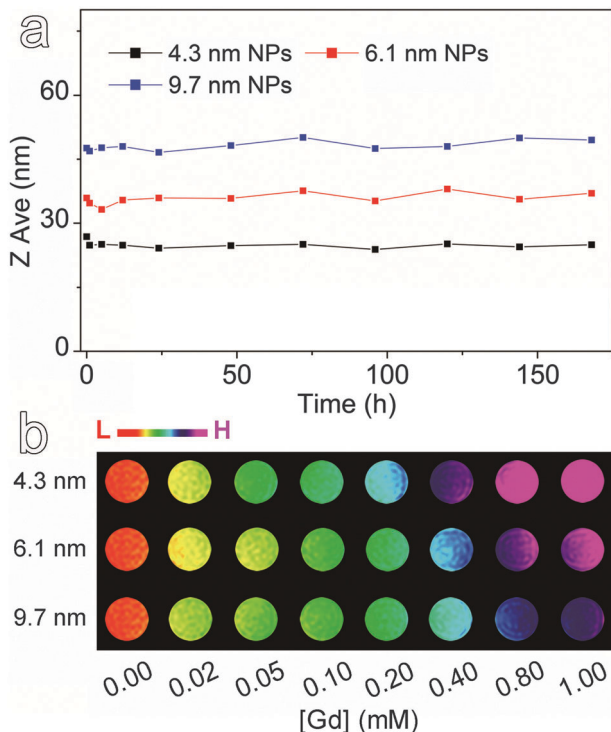


Fig. 2 Temporal evolutions of the hydrodynamic sizes of the PEGylated NaGdF<sub>4</sub>:Yb,Er nanoparticles in water (a), together with color-coded T<sub>1</sub>-weighted MR images of aqueous solutions containing the NaGdF<sub>4</sub>:Yb,Er nanoparticles with different Gd concentrations (b).

particles out of the reaction system. It is worth mentioning that the strong polarity of methanol may also help to activate the particle surface by encouraging the desorption of the surface capping ligand, yielding a higher growth rate.

It is also worth mentioning that the 4.3 nm NaGdF<sub>4</sub>:Yb,Er nanocrystals prepared in the absence of any low boiling point solvent exhibit clear upconversion luminescence as shown in Fig. 1e. Although the emissions are rather weak, the major peaks at around 521 nm, 541 nm and 655 nm, which can be typically attributed to radiative relaxations from the <sup>2</sup>H<sub>11/2</sub>, <sup>4</sup>S<sub>3/2</sub> and <sup>4</sup>F<sub>9/2</sub> states to the <sup>4</sup>I<sub>15/2</sub> state of Er<sup>3+</sup>, respectively, can be well identified. As expected, the integrated upconversion luminescence intensity is effectively enhanced by particle size, which can be interpreted by the reduced non-radiative relaxation pathways, as the percentage of the emitting ions on the particle surface decreases with the increase of particle size.<sup>7,22</sup>

To explore the application of the flow synthesized NaGdF<sub>4</sub>:Yb,Er nanocrystals as MRI contrast agents, three differently sized NaGdF<sub>4</sub>:Yb,Er nanocrystals (4.3 nm, 6.1 nm and 9.7 nm) were rendered water-soluble and biocompatible upon ligand exchange by using the polyethylene glycol (*M<sub>n</sub>* = 2000) ligand that bears a biphosphate group to replace the OA ligand.<sup>7,8</sup> The hydrodynamic properties of the resultant PEGylated NaGdF<sub>4</sub>:Yb,Er nanoparticles were carefully characterized. As shown in Fig. 2a, the PEGylated particles irrespective of the core size remain colloidal stable over one week, which is highly essential for *in vivo* applications.<sup>23</sup> The MRI contrast enhancement effects of the PEGylated

NaGdF<sub>4</sub>:Yb,Er nanoparticles are shown in Fig. 2b. In brief, all three particles show strong T<sub>1</sub> effects that decrease with the particle size, which is due to the reduced amount of contributing Gd<sup>3+</sup> as a consequence of the decreased specific surface area. By linear regression fitting of the experimental data shown in Fig. S3 (ESI<sup>†</sup>), the molar relaxivities *r*<sub>1</sub> of the 4.3 nm, 6.1 nm and 9.7 nm nanoparticles are extracted to be 3.5 mM<sup>-1</sup> s<sup>-1</sup>, 2.5 mM<sup>-1</sup> s<sup>-1</sup> and 1.3 mM<sup>-1</sup> s<sup>-1</sup> respectively.

In summary, flow synthesis has successfully been applied for synthesizing monodisperse magnetic/upconversion luminescent NaGdF<sub>4</sub>:Yb,Er nanocrystals with tunable size below 10 nm. Benefiting from the high pressure preparative conditions, hexagonally phased NaGdF<sub>4</sub>:Yb,Er nanocrystals as small as 4.3 nm were obtained. More importantly, the high pressure also allowed the use of low boiling point solvents such as cyclohexane and methanol as a co-solvent, which offered flexibility for further tuning the particle size up to 10 nm without sacrificing the particle size monodispersity through reducing the viscosity and/or increasing the solubility of the precursors. The excellent monodispersity of the particles thus provides an opportunity to balance the MRI contrast enhancement effect upon further biocompatible surface modification and the upconversion luminescence intensity for multimodality imaging applications, as these two properties present reverse particle size dependencies. In conclusion, the current investigations have paved a novel and reliable approach for preparing rare-earth nanocrystals with controlled size and properties, which is highly desirable for practical applications of rare-earth nanocrystals, owing to the probable large-scale production.

This work was supported by NSFC (81530057, 21403250, 81471726, 21321063), and CAS (2016YZ01, CMS-PY-201314).

## Notes and references

- 1 C. Y. Liu, Y. Hou and M. Y. Gao, *Adv. Mater.*, 2014, **26**, 6922–6932.
- 2 W. Zheng, P. Huang, D. Tu, E. Ma, H. Zhu and X. Chen, *Chem. Soc. Rev.*, 2015, **44**, 1379–1415.
- 3 H. Dong, S. Du, X. Zheng, G. Lyu, L. Sun, L. Li, P. Zhang, C. Zhang and C. Yan, *Chem. Rev.*, 2015, **115**, 10725–10815.
- 4 S. Gai, C. Li, P. Yang and J. Lin, *Chem. Rev.*, 2014, **114**, 2343–2389.
- 5 X. Ai, C. J. H. Ho, J. Aw, A. B. E. Attia, J. Mu, Y. Wang, X. Wang, Y. Wang, X. Liu, H. Chen, M. Y. Gao, X. Chen, E. K. L. Yeow, G. Liu, M. Olivo and B. Xing, *Nat. Commun.*, 2016, **7**, 10432–10440.
- 6 J. Huang, Y. Hou, C. Liu, L. Jing, T. Ma, X. Sun and M. Y. Gao, *Chem. Mater.*, 2015, **27**, 7918–7925.
- 7 C. Liu, Z. Gao, J. Zeng, Y. Hou, F. Fang, Y. Li, R. Qiao, L. Shen, H. Lei, W. Yang and M. Y. Gao, *ACS Nano*, 2013, **7**, 7227–7240.
- 8 Y. Hou, R. Qiao, F. Fang, X. Wang, C. Dong, K. Liu, C. Liu, Z. Liu, H. Lei, F. Wang and M. Y. Gao, *ACS Nano*, 2013, **7**, 330–338.
- 9 J. Zhou, Y. Sun, X. Du, L. Xiong, H. Hu and F. Li, *Biomaterials*, 2010, **31**, 3287–3295.
- 10 R. Qiao, C. Liu, M. Liu, H. Hu, C. Liu, Y. Hou, K. Wu, Y. Lin, J. Liang and M. Y. Gao, *ACS Nano*, 2015, **9**, 2120–2129.
- 11 G. Wang, Q. Peng and Y. Li, *Acc. Chem. Res.*, 2011, **44**, 322–332.
- 12 F. Wang, Y. Han, C. S. Lim, Y. Lu, J. Wang, J. Xu, H. Chen, C. Zhang, M. Hong and X. Liu, *Nature*, 2010, **463**, 1061–1065.
- 13 N. J. J. Johnson, W. Oakden, G. J. Stanis, R. Scott Prosser and F. C. J. M. van Veggel, *Chem. Mater.*, 2011, **23**, 3714–3722.
- 14 Z. Li, Y. Zhang and S. Jiang, *Adv. Mater.*, 2008, **20**, 4765–4769.
- 15 H. Xing, S. Zhang, W. Bu, X. Zheng, L. Wang, Q. Xiao, D. Ni, J. Zhang, L. Zhou, W. Peng, K. Zhao, Y. Hua and J. Shi, *Adv. Mater.*, 2014, **26**, 3867–3872.

- 16 X. Li, R. Wang, F. Zhang and D. Zhao, *Nano Lett.*, 2014, **14**, 3634–3639.
- 17 M. Jiao, J. Zeng, L. Jing, C. Liu and M. Y. Gao, *Chem. Mater.*, 2015, **27**, 1299–1305.
- 18 C. Liu, Y. Qi, R. Qiao, Y. Hou, K. Chan, Z. Li, J. Huang, L. Jing, J. Du and M. Y. Gao, *Nanoscale*, 2016, DOI: 10.1039/C5NR07858J.
- 19 Q. Jia, J. Zeng, R. Qiao, L. Jing, L. Peng, F. Gu and M. Y. Gao, *J. Am. Chem. Soc.*, 2011, **133**, 19512–19523.
- 20 S. G. Kwon and T. Hyeon, *Small*, 2011, **7**, 2685–2702.
- 21 K. De Nolf, R. K. Capek, S. Abe, M. Sluydts, Y. Jang, J. C. Martins, S. Cottenier, E. Lifshitz and Z. Hens, *J. Am. Chem. Soc.*, 2015, **137**, 2495–2505.
- 22 F. Wang and X. Liu, *Chem. Soc. Rev.*, 2009, **38**, 976–989.
- 23 Z. Gao, T. Ma, E. Zhao, D. Docter, W. Yang, R. H. Stauber and M. Y. Gao, *Small*, 2016, **12**, 556–576.